Received: 20 May 2021 | Revised: 24 June 2021 | Accepted: 25 June 2021

DOI: 10.1111/cas.15050

ORIGINAL ARTICLE

Cancer Science WILEY

NKG2D defines tumor-reacting effector CD8$^+$ T cells within tumor microenvironment

Marija Mojic[1] | Kiyomi Shitaoka[2] | Chikako Ohshima[1] | Sisca Ucche[1] | Fulian Lyu[2] | Hiroshi Hamana[2] | Hideaki Tahara[3,4] | Hiroyuki Kishi[2] | Yoshihiro Hayakawa[1]

[1]Institute of Natural Medicine, University of Toyama, Toyama, Japan

[2]Department of Immunology, Graduate School of Medicine and Pharmaceutical Sciences (Medicine), Toyama, Japan

[3]The, Institute of Medical Science, The University of Tokyo, Tokyo, Japan

[4]Department of Cancer Drug Discovery and Development, Research Center, Osaka International Cancer Institute, Osaka, Japan

Correspondence
Yoshihiro Hayakawa, Institute of Natural Medicine, University of Toyama, Sugitani 2630, Toyama, Toyama 930-0194, Japan.
Email: haya@inm.u-toyama.ac.jp

Funding information
Ministry of Education, Culture, Sports, Science and Technology, Grant/Award Number: 17H06398; Yasuda Memorial Medical Foundation, Grant/Award Number: Research grant 2020

Abstract

For successful immunotherapy for cancer, it is important to understand the immunological status of tumor antigen-specific CD8$^+$ T cells in the tumor microenvironment during tumor progression. In this study, we monitored the behavior of B16OVA-Luc cells in mice immunized with a model tumor antigen ovalbumin (OVA). Using bioluminescence imaging, we identified the time series of OVA-specific CD8$^+$ T-cell responses during tumor progression: initial progression, immune control, and the escape phase. As a result of analyzing the status of tumor antigen-specific CD8$^+$ cells in those 3 different phases, we found that the expression of NKG2D defines tumor-reacting effector CD8$^+$ T cells. NKG2D may control the fate and TOX expression of tumor-reacting CD8$^+$ T cells, considering that NKG2D blockade in OVA-vaccinated mice delayed the growth of the B16OVA-Luc2 tumor and increased the presence of tumor-infiltrating OVA-specific CD8$^+$ T cells.

KEYWORDS
cytotoxic T cell, immune surveillance, NKG2D, TOX, tumor microenvironment

1 | INTRODUCTION

Tumor-specific CD8$^+$ T cells play a central role in immune surveillance for cancer. There are positive associations between the presence of CD8$^+$ T cells in the tumor microenvironment (TME) and clinical disease outcomes;[1-3] therefore, CD8$^+$ T cells in TME are considered a good prognostic marker in various cancer types. In TME, however, the activation of tumor-specific CD8$^+$ T cells through their recognition of tumor-specific antigens is often impaired by negative regulators. Immune-checkpoint molecules, such as PD-1 and CTLA-4, are the targets of those negative regulators of T cells, and immune-checkpoint blockers (ICBs) are known to restore the anti-tumor effector function of CD8$^+$ T cells to exert therapeutic effects in many cancer patients.[4–8] Although patients may show a strong response to ICBs, the clinical outcomes of this therapy are often limited because there is marked variation in the immunological status of CD8$^+$ T cells, the mutation and antigen status of tumors, and the clinical history and host genetic background of cancer patients.[9,10] For successful immunotherapy for cancer, it is important to understand the immunological status of tumor antigen-specific CD8$^+$ T cells in TME during tumor progression. However, it is difficult to assess temporal changes in CD8$^+$ T cells within the tumor microenvironment in a clinical setting because accessibility to serial tumor biopsies is not feasible. Therefore, we must experimentally examine how tumor antigen-specific CD8$^+$ T cells change their immunological status along with the progression of tumors in pre-clinical cancer models.

In this study, we established a bioluminescence imaging model to monitor the interplay between occult immunogenic tumor and host anti-tumor immunity. Using mouse B16 melanoma cells expressing ovalbumin (OVA) and luciferase (B16OVA-Luc cells), we monitored

the exact behavior of B16OVA-Luc cells in mice immunized with a model tumor antigen OVA to clarify the time scale of the specific immune response to control occult tumors. We further analyzed the status of tumor antigen-specific $CD8^+$ T cells in different phases of immunological surveillance during tumor progression and identified NKG2D as a marker of tumor-reacting effector $CD8^+$ T cells.

2 | MATERIALS AND METHODS

2.1 | Cells

Murine melanoma cell line constitutively expressing ovalbumin, B16OVA (MO4) was a kind gift from Dr. Shinichiro Fujii (Riken, Japan). B16OVA-Luc2 cells stably expressing luciferase with the cytomegalovirus (CMV) promoter were established in accordance with a previously described method.[11] pGL4.50 [luc2/CMV/Hygro] vector and D-luciferin were purchased from Promega (Madison, WI, USA), Lipofectamine 2000 was obtained from Invitrogen (Carlsbad, CA, USA), and hygromycin B was obtained from Nacalai Tesque (Kyoto, Japan). In vitro and in vivo characterizations of B16OVA-Luc2 cells are shown in Figure S1. There was a positive correlation between the luminescence (photons/sec) and cell number (Figure S1A, $R^2 = 0.9907$). Cells were cultured for no longer than a month, and not reauthenticated.

2.2 | Mice

Six- to 8-wk-old wild-type C57BL/6J (WT) mice were purchased from CLEA Japan, Inc (Tokyo, Japan). Interferon-$\gamma^{-/-}$ (IFN-γ KO) mice with a C57BL/6 background were kindly provided by Dr. Yoichiro Iwakura (Tokyo University of Science, Chiba, Japan) and maintained at the Laboratory Animal Research Center, Institute of Medical Science, the University of Tokyo. All experiments were approved and performed in accordance with the guidelines of Care and Use of Laboratory Animals of University of Toyama and the Animal Care and Use Committee of Institute of Medical Science of the University of Tokyo.

2.3 | Bioluminescence imaging of in vivo cancer cell growth

Mice were inoculated subcutaneously (sc) with B16OVA-Luc2 cells and tumor growth was monitored by bioluminescence imaging. To obtain bioluminescence images, mice were injected with D-luciferin (Promega, 150 mg/kg ip) and luminescence was measured with an in vivo imaging system (IVIS Lumina II, Perkin Elmer, MA, USA) 20 min after the D-luciferin injection. Regions of interest analyses were performed using Living Image 4.2 Software (Caliper Life Science, Hopkinton, MA, USA) to determine the light emitted from the tumor. For each mouse, all values were determined as photons per sec (photon/sec). Representative data on bioluminescence imaging (Figure S1B), a summary of tumor growth represented as luminescence (Figure S1C) are shown. The group of mice received sc injections of 100 μg of chicken ovalbumin protein (OVA, Sigma) emulsified in complete Freund's adjuvant (CFA, Sigma) or incomplete Freund's adjuvant (IFA, Sigma) 14 d (OVA-CFA) or 7 d (OVA-IFA) prior to tumor inoculation. In some experiments, mice were treated with ip injections of 250 μg of anti-IFN-γ (clone H-22, Bio X Cell), anti-CD8 (clone 53.6.2, Bio X Cell), or anti-NKG2D (clone HMG2D, Bio X Cell).

2.4 | Tumor-infiltrating lymphocyte (TIL) isolation and flow cytometry

Tumor samples were cut into small pieces and digested in serum-free RPMI 1640 medium containing 2 mg/mL collagenase (Roche Diagnostics GmbH) and 0.1 mg/mL DNase I (Roche Diagnostics GmbH) for 1 h at 37°C.[12] A single-cell suspension from tumor-draining axillary lymph nodes was prepared by mincing and filtration. Samples were pre-incubated with anti-CD16/32 (2.4G2) to avoid non-specific binding of antibodies to FcγR. For enumeration and characterization of tumor-specific $CD8^+$ T cells in TIL, we used OVATet, a fluorochrome-conjugated complex of 4 MHC class I molecules each bound to the MHC I–restricted dominant SIINFEKL OVA epitope (MBL). After incubation with OVATet, samples were further stained with a saturating amount of the fluorophore-labeled antibodies for cell-surface staining: anti-mouse CD3ε (2C11, BD Pharmingen or Tonbo Biosciences), NK1.1 (PK136, BD Pharmingen), CD4 (GK1.5, Tonbo Biosciences), CD279/PD-1 (RMP1-30, eBioscience), CD233/LAG3 (C9B7W, eBioscience), CD366/TIM-3 (8B.2C12, eBioscience), and CD314/NKG2D (CX5, BioLegend). For intracellular staining, cells were fixed and permeabilized in accordance with the manufacturer's instructions (FoxP3/Transcription factor staining buffer set, eBioscence) before being stained with fluorophore-labeled antibodies: anti-mouse eomesodermin (Eomes, clone REA116, MACS Miltenyi Biotec), T-bet (4B10, BioLegend), and TOX (REA473, Miltenyi Biotec). Flow cytometry was performed with FACS Canto (BD Biosciences) and data were analyzed with FlowJo software (Tree Star).

2.5 | Single-cell RT-PCR and sequencing

Tumor samples were isolated 12 and 19 d after tumor inoculation, and subjected to a single-cell TCR β-chain CDR3 repertoire analysis as previously described with some modifications.[13,14] Briefly, 5 μL of the RT-PCR mix was added to each well containing a single T cell, and 1-step RT-PCR was performed. The program for the 1-step RT-PCR was as follows: 40 min at 45°C for the RT reaction, 98°C for 1 min and 30 cycles of 98°C for 10 s, 52°C for 5 s, and 72°C for 1 min. The resultant 1-step RT-PCR products were diluted 10-fold with nuclease-free water and used for a second cycle of PCR. To amplify the cDNA of the TCRβ, 2 μL of the diluted 1-step RT-PCR products

were added to each well of a new 96-well PCR plate containing 18 μL of the 2nd-PCR β mix. The PCR program for the second PCR cycle was as follows: 98°C for 1 min and 35 cycles of 98°C for 10 s, 52°C for 5 s, and 72°C for 30 s. The TCR repertoire was analyzed with the IMGT/V-Quest tool (http://www.imgt.org/).[15] The clonality index was calculated using mathematical equations, as described.[16]

2.6 | In vivo BrdU uptake

Mice were injected ip with 1 mg of BrdU (Wako) twice per day (10-12 h apart) starting from 2 d before scheduled tumor excision. Single-cell suspensions of TIL from harvested tumors were stained for CD3ε, CD4, and OVATet, after which they were stained for intracellular BrdU incorporation in accordance with the manufacturer's instructions (BrdU Flow Kit; BD Biosciences). Non-BrdU-treated mice were included in the experiment as a negative control.

2.7 | Statistical analysis

All data were obtained from the groups of 5-10 mice and are representative of at least 2 independent experiments. Statistical comparisons between 2 groups were performed using Student *t* test. One-way analysis of variance (ANOVA) with Bonferroni correction was used to compare 3 or more groups. A *P*-value equal to or <.05 was considered significant.

3 | RESULTS

3.1 | Identification of the immune control phase of B16OVA-Luc2 growth in OVA-vaccinated mice

To identify the immune control phase of tumor growth by antigen-specific T cells, we monitored the luminescence of B16OVA-Luc2 cells implanted in control B6 mice (control) or B6 mice vaccinated with OVA (Vaccinated). Although B16OVA-Luc2 cells aggressively grew in the control B6 mice, these cells showed biphasic growth in OVA-vaccinated mice (Figure 1A). In OVA-vaccinated mice, the growth of B16OVA-Luc2 cells initially progressed (Days 2 to 8), then was stable or declined (Days 10 to 12), and thereafter showed secondary progression (from Day 16 and thereafter). As shown in the Figure S1C, the palpable and visible tumor to measure the size was not technically possible until day 8 to 10. Therefore, the bioluminescence imaging was capable of detecting and quantifying the cancer cell-derived luminescence immediately after the inoculation and monitor the exact behavior of B16OVA-Luc cells under the different immunological conditions. Such biphasic tumor growth may be controlled by $CD8^+$ T cells and host IFN-γ production because it was compromised in OVA-vaccinated IFN-γ KO mice, OVA-vaccinated WT mice treated with IFN-γ-blocking antibody, or OVA-vaccinated WT mice treated with a depleting anti-CD8 antibody (Figure S1). Importantly, B16OVA-Luc cells lost their OVA expression throughout the immune control in OVA-immunized mice (data not shown). These results clearly indicated that the biphasic in vivo growth of B16OVA-luc2 tumors in OVA-vaccinated mice was controlled by IFN-γ- and $CD8^+$ T-cell-dependent anti-tumor immune responses.

3.2 | Clonal expansion of tumor antigen-specific $CD8^+$ T cells associated with immune control of B16OVA-Luc2 growth

To understand the status of antigen-specific T cells within the tumor microenvironment in the 3 different phases of B16OVA-Luc2 tumor growth: initial progression (Days 0 to 8), immune control (Days 10-12), and escape (Day 16 and thereafter) phases as determined by temporal bioluminescence imaging (Figure 1A), we analyzed TILs using flow cytometry at 8, 12, and 19 days after tumor inoculation. The proportion of OVA-specific $CD8^+$ T cells (determined as OVA-$tetramer^+$ $CD4^-$ T cells, referred to $OVATet^+$ T cells from this point forwards) were markedly increased in the tumors of OVA-vaccinated mice during the immune control phase compared with naïve mice (Figure 1B). Both the frequency of $OVATet^+$ T cells (Figure 1C) and intensity of OVA-tetramer staining (Figure 1D) were significantly increased on Day 12, when tumor growth was actively controlled by T cells, whereas they declined on Day 19 along with the progressive growth of B16OVA-Luc2 tumors (Figure 1C, D). Using single-cell TCR β chain CDR3 analysis,[13] the TCR repertoire of OVA-specific T cells on Days 12 and 19 were examined. As shown in Figure 1E, the clonality index of the TCR repertoire of $OVATet^+$ T cells was largely increased on Day 12 in OVA-vaccinated mice compared with the control, whereas it had decreased by Day 19 to the control level. Consistent with the clonality of the TCR repertoire, the proliferation of $OVATet^+$ T cells was also significantly increased on Day 12 as determined by in vivo BrdU uptake, and decreased on Day 19 (Figure 1F). Collectively, these results suggested that the loss of the OVA-specific $CD8^+$ T-cell response in the tumor microenvironment correlated with the progressive growth of B16OVA-Luc2 tumors.

3.3 | Increased expression of NKG2D in tumor-reacting $CD8^+$ T cells at the immune control effector phase

Next, we examined whether the expression of immune regulatory molecules is associated with the functional status of tumor-specific $CD8^+$ T cells in the immune control phase (Days 10-12). As shown in Figure S3, neither PD-1, LAG3, nor TIM-3 expression in $OVATet^+$ T cells was associated with the progression of B16OVA-Luc2 tumor growth. Instead of those immune-checkpoint molecules, the expression of NKG2D in the tumor-infiltrating $OVATet^+$ T cells was found to be associated with the immune control of B16OVA-Luc2 tumor growth (Figure 2A, B). Not only the intensity of NKG2D expression, but also the proportion of $NKG2D^+$ cells in $OVATet^+$ T cells were

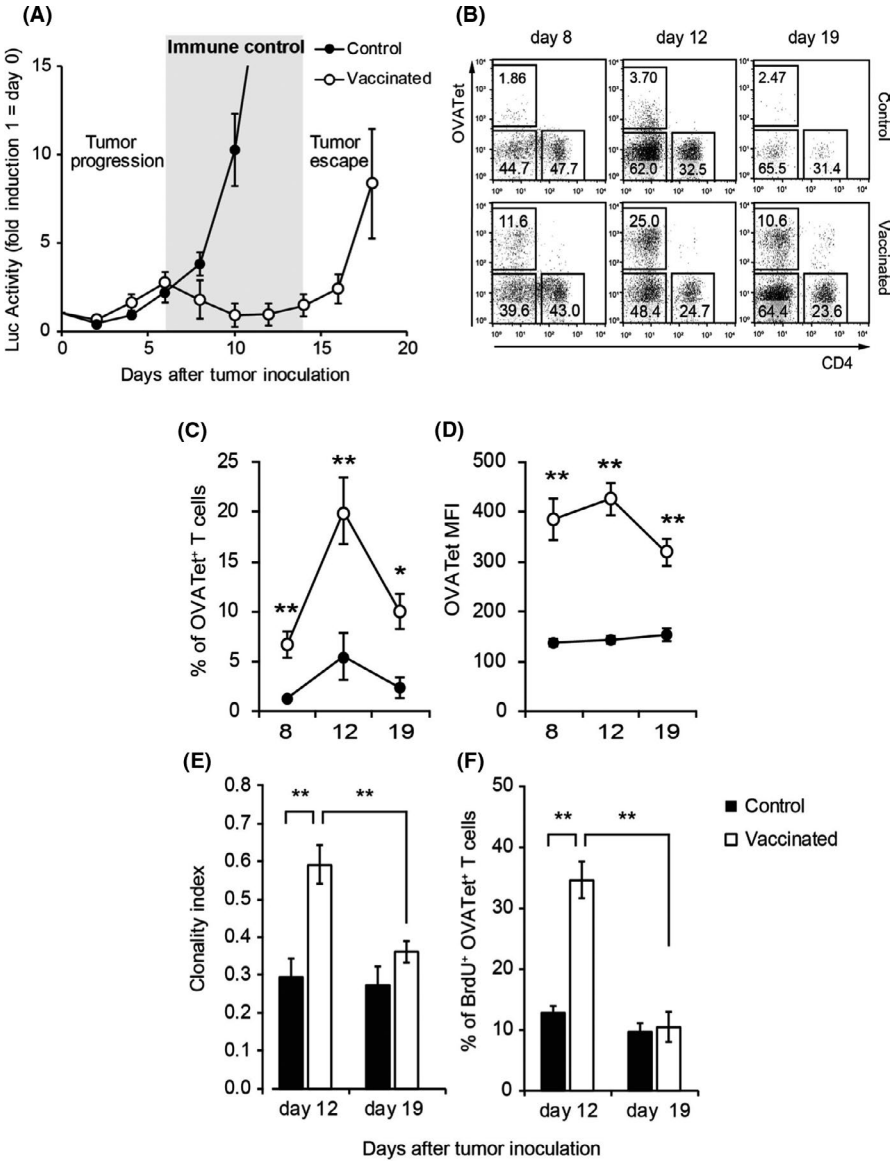

FIGURE 1 Identification of the immune control phase of B16OVA-Luc2 growth in OVA-vaccinated mice B16OVA-Luc2 cells (10^5 cells/mouse) were used to sc inoculate untreated (Control) or OVA-vaccinated (Vaccinated) B6 mice, and the growth of B16OVA-Luc2 cells was monitored by bioluminescence imaging (A). At the indicated time-points, TIL were collected and subjected to flow cytometry (Day 0 = tumor inoculation). Dot plots of flow cytometry electronically gated on $NK1.1^-CD3^+$ lymphocytes are shown (B). The numbers are the percentages of cells in each gate. A summary of the percentage of $OVATet^+$ T cells (C) or the mean fluorescence intensity (MFI) of OVATet staining (D) is shown. The clonality index of $OVATet^+$ T-cell infiltrating tumors on the indicated days is shown (E). A summary of the in vivo BrdU uptake of $OVATet^+$ T cells is shown (F). Data are presented as the mean ± SEM. $^{**}P < .01$

higher in the immune control phase (Days 8 to 12). Such NKG2D expression was predominant in $OVATet^+$ (tumor-reacting) T cells, but not in other tumor-infiltrating T cells (Figure 2B). Importantly, the expression of NKGD was specifically increased in the tumor-infiltrating OVA-specific T cells, because $OVATet^+$ T cells in tumor-draining lymph nodes did not show any increase in their NKG2D expression (Figure 2C). These results suggested that NKG2D expression defines tumor-reacting effector $CD8^+$ T cells in the immune control effector phase.

3.4 | NKG2D controls tumor-reacting $CD8^+$ T-cell fate and TOX expression

Given that NKG2D is known to regulate $CD8^+$ T-cell fate through transcriptional control, we next examined the expression of transcription factors that are known to regulate $CD8^+$ T-cell effector and memory states. The expressions of T-box transcription factors Eomes and T-bet in tumor-reacting $OVATet^+$ T cells were higher (Eomes, Figure 3A) or unchanged (T-bet, Figure 3B), whereas the population of $OVATet^+$ T cells with highly expressing thymocyte selection-associated high mobility group box (TOX) was markedly increased in the immune control phase (Day 11). The induction of $TOX^{hi}NKG2D^+OVATet^+$ T cells was specific to the T-cell population residing within the tumor (Figure 3C). To further determine whether NKG2D and TOX had functional role in the control of tumor-reacting $CD8^+$ T cells, the OVA-vaccinated mice were treated with anti-NKG2D (clone HMG2D) blocking antibody. By blocking NKG2D in OVA-vaccinated mice, B16OVA-Luc2 tumor growth was delayed (Figure 4A), and the presence of tumor-infiltrating $OVATet^+$ T cells was increased compared with the control mice (Figure 4B). Of note, the delayed treatment with anti-NKG2D (starting from day 6) was also effective (data not shown). Along with the better control of B16OVA-Luc2 tumor growth, $TOX^{hi}OVATet^+$ T cells were more dominant in tumors treated with anti-NKG2D (Figure 4C). These results suggested that NKG2D

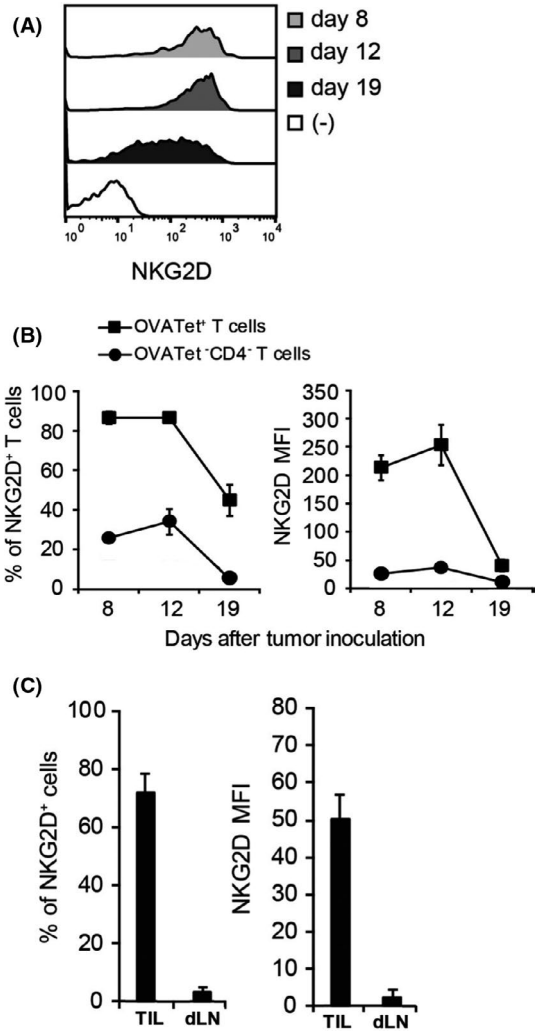

FIGURE 2 Increased expression of NKG2D in tumor-reacting CD8$^+$ T cells in the immune control effector phase. B16OVA-Luc2 cells (10^5 cells/mouse) were used to sc inoculate vaccinated C57BL/6 mice. At the indicated time-points, TIL were collected and subjected to flow cytometry (Day 0 = tumor inoculation). A, Representative histograms of NKG2D expression on OVATet$^+$ T cells at the indicated time-points are shown (control (–): isotype control). B, The percentage of NKG2D$^+$ T cells (left panel) or the mean fluorescence intensity (MFI) of NKG2D staining (right panel) on the indicted T-cell population is shown. C, On Day 11, TIL or tumor-draining axillary lymph nodes (dLN) were collected and subjected to flow cytometry. The percentage of NKG2D$^+$ T cells (left panel) or mean fluorescence intensity (MFI) of NKG2D staining (right panel) on the OVATet$^+$ T cells isolated from the indicated sources are shown. Data are presented as the mean ± SEM

controls the fate and TOX expression of tumor-reacting CD8$^+$ T cells in TME.

4 | DISCUSSION

In this study, we monitored the behavior of B16OVA-Luc cells in mice immunized with a model tumor antigen, OVA. Using bioluminescence imaging, we identified the time series of OVA-specific

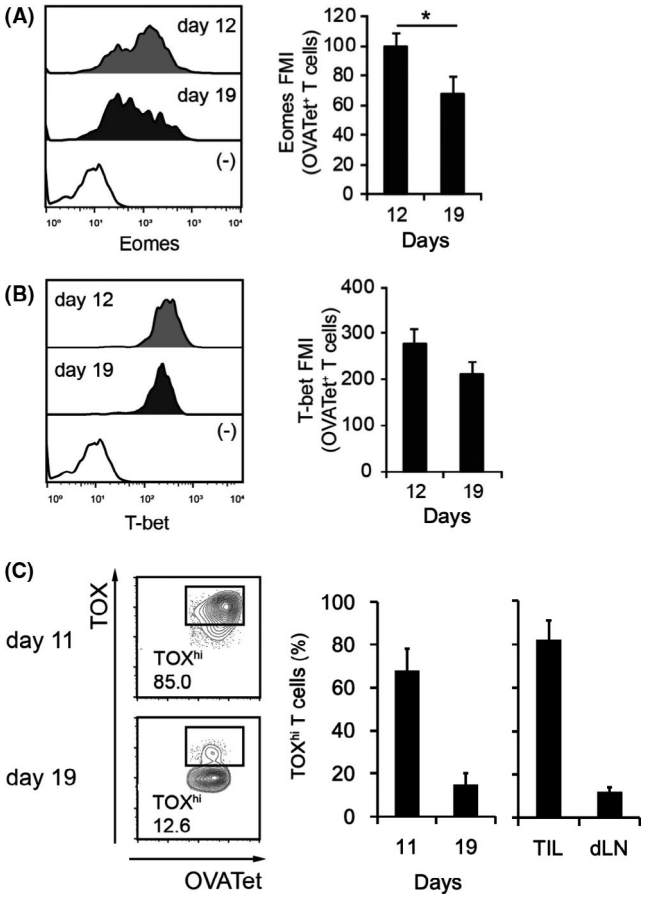

FIGURE 3 Expression of transcription factors in tumor antigen-specific CD8$^+$ T cells in the immune control effector phase. B16OVA-Luc2 cells (10^5 cells/mouse) were used to sc inoculate vaccinated C57BL/6 mice. B16OVA-Luc2 cells (10^5 cells/mouse) were used to sc inoculate vaccinated C57BL/6 mice. At the indicated time-points, TIL were collected and subjected to flow cytometry (Day 0 = tumor inoculation). Representative histograms (left) and summaries (right) of Eomes (A) and T-bet (B) expression in OVATet$^+$ T cells are shown. C, Representative contour plots (left) and summaries (middle) of TOX expression (TOX^{hi}) on OVATet$^+$ T cells in TIL are shown. The percentage of TOX^{hi}OVATet$^+$ T cells isolated from the indicated sources is shown (right). Data are presented as the mean ± SEM

CD8$^+$ T-cell responses during tumor progression: initial progression, immune control, and the escape phase. As a result of analyzing the status of tumor antigen-specific CD8$^+$ T cells in those 3 different phases, we found that the expression of NKG2D defines tumor-reacting effector CD8$^+$ T cells within TME. NKG2D may control the fate and TOX expression of tumor-reacting CD8$^+$ T cells considering that NKG2D blockade in OVA-vaccinated mice delayed the growth of B16OVA-Luc2 tumors and increased the presence of tumor-infiltrating OVA-specific CD8$^+$ T cells in TME.

NKG2D is an activating receptor expressed on NK cells, NKT cells, γδ cells, and a subset of activated CD8$^+$ T cells (Wensveen et al, 2018). In CD8$^+$ T cells, NKG2D is known to function as a co-stimulatory molecule to enhance their TCR-mediated effector functions.[17–19] NKG2D signaling is also known to activate the memory-associated

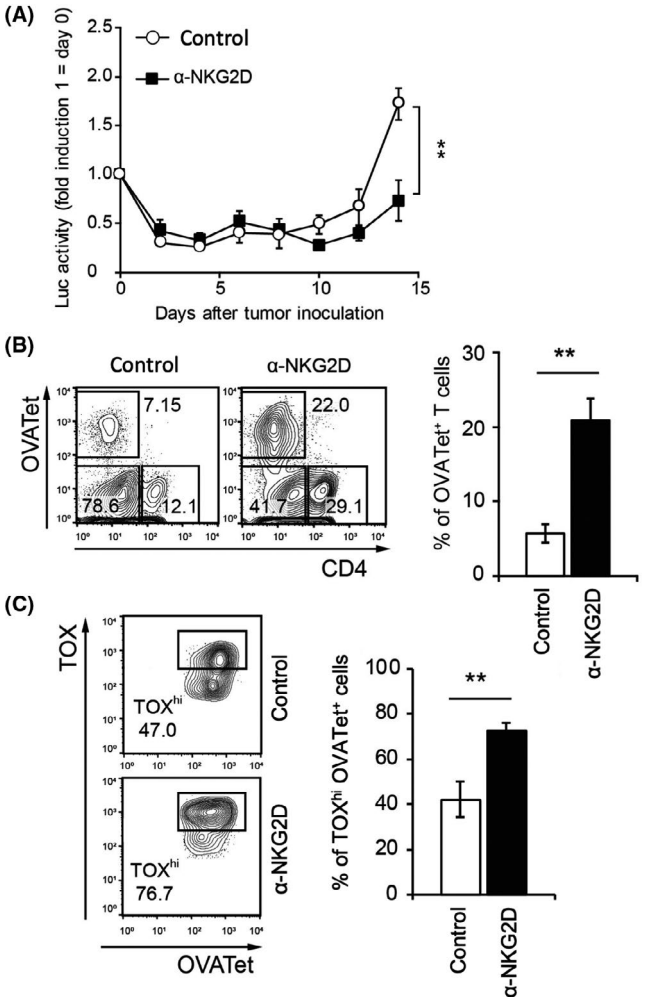

FIGURE 4 NKG2D controls tumor-reacting $CD8^+$ T-cell fate and TOX expression. B16OVA-Luc2 cells (10^5 cells/mouse) were used to sc inoculate vaccinated C57BL/6 mice that were treated with anti-NKG2D antibody (clone HMG2D, 250 μg/mouse, ip) every 3 d starting from Day 0 (tumor inoculation day) or were left untreated. A, Bioluminescence of B16OVA-Luc2 tumors was monitored every other day and normalized by luminescence measured for individual tumors on Day 0. Tumors were collected on Day 16 for TIL analysis using flow cytometry. B, Representative contour plots of TIL electronically gated on $NK1.1^-CD3^+$ T cells (left) and a summary of the percentage of $OVATet^+$ T cells in tumors (right) are shown. C, Representative contour plots of TIL electronically gated on $OVATet^+CD4^-$ T cells (left) and a summary of $TOX^{hi}OVATet^+$ T cells in tumors (right) are shown. Data are presented as the mean ± SEM. $^{**}P < .01$

transcription factor Eomes, possibly through the regulation of the mTORC1 pathway,[20] and to contribute to memory formation of $CD8^+$ T cells by enhancing the IL-15-mediated PI3K signaling pathway.[21,22] Regarding the expression of NKG2D in $CD8^+$ T cells, it has been reported that $CD8^+$ effector memory T cells present in vitiligo skin increase their NKG2D expression by an IL-15-dependent mechanism.[23] Interestingly, the temporal blockade of NKG2D during the effector phase resulted in the formation of defective memory $CD8^+$ T cells, potentially through altering T-cell transcriptional and epigenetic programs.[24] Contrary to those co-stimulatory functions of NKG2D, our results suggested that it paradoxically functions as a potential negative regulator of tumor-reacting $CD8^+$ T cells in TME. Alternatively, NKG2D expression may be associated with the dysfunction of tumor-specific $CD8^+$ T cells. Indeed, the dysfunction of $CD8^+$ T cells is considered as a differentiation state distinct from their effector or memory state in the context of anti-tumor immune responses.[25–30] Recently, the transcription factor TOX was found to be a crucial regulator of the differentiation of tumor-specific T cells into the dysfunction or exhaustion state. Expression of TOX was driven by chronic T-cell receptor stimulation and NFAT activation[31,32] and such TOX expression resulted in a commitment to the exhaustion of T cells induced by the persistent antigen-dependent TCR stimulation. It is also suggested that TOX-dependent exhaustion may prevent the overstimulation of T cells; therefore, rescue of antigen-reacting T cells from the activation-induced cell death occurred upon chronic antigen stimulation. Although the exact role of co-stimulatory molecules in TOX expression in $CD8^+$ T cells is unclear, our results suggested the potential role of NKG2D in regulating TOX expression in antigen-specific $CD8^+$ T cells in TME. The presence of antigen-specific $CD8^+$ T cells and their expression of TOX were increased by blocking NKG2D; therefore, NKG2D may negatively regulate the expression of TOX in tumor-reacting effector $CD8^+$ T cells. Alternatively, NKG2D may be involved in determining the tumor-reacting $TOX^{hi}CD8^+$ T-cell fate in differentiating to TOX^{lo} cells. Further studies are clearly needed to understand the mechanism of how NKG2D contributes to the decision on the fate of tumor-reacting $CD8^+$ effector T cells and the relevance of TOX.

ACKNOWLEDGMENTS

We are grateful to Sanae Hirota, Asuka Asami, and Setsuko Nakayama for their technical assistance. This study was partly supported by a Grant-in-Aid for Scientific Research on Innovative Areas (17H06398), The Ministry of Education, Culture, Sports, Science and Technology (MEXT), Japan (YH), Yasuda Memorial Medical Foundation, and the Cooperative Research Project from the Institute of Natural Medicine, University of Toyama.

DISCLOSURE

None of the authors have conflicts of interest to declare.

ORCID

Hideaki Tahara https://orcid.org/0000-0002-1735-5372
Yoshihiro Hayakawa https://orcid.org/0000-0002-7921-1171

REFERENCES

1. Kim PS, Ahmed R. Features of responding T cells in cancer and chronic infection. *Curr Opin Immunol*. 2010;22:223-230.
2. Kmiecik J, Poli A, Brons NHC, et al. Elevated CD3+ and CD8+ tumor-infiltrating immune cells correlate with prolonged survival in glioblastoma patients despite integrated immunosuppressive mechanisms in the tumor microenvironment and at the systemic level. *J Neuroimmunol*. 2013;264:71-83.
3. Piersma SJ, Jordanova ES, van Poelgeest MIE, et al. High number of intraepithelial CD8+ tumor-infiltrating lymphocytes is associated

with the absence of lymph node metastases in patients with large early-stage cervical cancer. *Cancer Res*. 2007;67:354.
4. Wei SC, Duffy CR, Allison JP. Fundamental mechanisms of immune checkpoint blockade therapy. *Cancer Discov*. 2018;8:1069.
5. Pardoll DM. The blockade of immune checkpoints in cancer immunotherapy. *Nat Rev Cancer*. 2012;12:252-264.
6. Butler NS, Nolz JC, Harty JT. Immunologic considerations for generating memory CD8 T cells through vaccination. *Cell Microbiol*. 2011;13:925-933.
7. Kaech SM, Cui W. Transcriptional control of effector and memory CD8+ T cell differentiation. *Nat Rev Immunol*. 2012;12:749-761.
8. Slaney CY, Kershaw MH, Darcy PK. Trafficking of T cells into tumors. *Cancer Res*. 2014;74:7168.
9. Kalbasi A, Ribas A. Tumour-intrinsic resistance to immune checkpoint blockade. *Nat Rev Immunol*. 2020;20:25-39.
10. Pitt Jonathan M, Vétizou M, Daillère R, et al. Resistance mechanisms to immune-checkpoint blockade in cancer: tumor-intrinsic and -extrinsic factors. *Immunity*. 2016;44:1255-1269.
11. Takahashi K, Nagai N, Ogura K, et al. Mammary tissue microenvironment determines T cell-dependent breast cancer-associated inflammation. *Cancer Sci*. 2015;106:867-874.
12. Ogura K, Sato-Matsushita M, Yamamoto S, et al. NK Cells control tumor-promoting function of neutrophils in mice. *Cancer Immunol Res*. 2018;6:348-357.
13. Kobayashi E, Mizukoshi E, Kishi H, et al. A new cloning and expression system yields and validates TCRs from blood lymphocytes of patients with cancer within 10 days. *Nat Med*. 2013;19:1542-1546.
14. Hamana H, Shitaoka K, Kishi H, Ozawa T, Muraguchi A. A novel, rapid and efficient method of cloning functional antigen-specific T-cell receptors from single human and mouse T-cells. *Biochem Biophys Res Commun*. 2016;474:709-714.
15. Giudicelli V, Chaume D, Lefranc M-P. IMGT/V-QUEST, an integrated software program for immunoglobulin and T cell receptor V-J and V–D–J rearrangement analysis. *Nucleic Acids Res*. 2004;32:W435-W440.
16. Kargl J, Busch SE, Yang GHY, et al. Neutrophils dominate the immune cell composition in non-small cell lung cancer. *Nat Commun*. 2017;8:14381.
17. Ehrlich LIR, Ogasawara K, Hamerman JA, et al. Engagement of NKG2D by cognate ligand or antibody alone is insufficient to mediate costimulation of human and mouse $CD8^+$ T cells. *J Immunol*. 2005;174:1922.
18. Groh V, Rhinehart R, Randolph-Habecker J, Topp MS, Riddell SR, Spies T. Costimulation of CD8αβ T cells by NKG2D via engagement by MIC induced on virus-infected cells. *Nat Immunol*. 2001;2:255-260.
19. Prajapati K, Perez C, Rojas LBP, Burke B, Guevara-Patino JA. Functions of NKG2D in CD8+ T cells: an opportunity for immunotherapy. *Cell Mol Immunol*. 2018;15:470-479.
20. McQueen B, Trace K, Whitman E, Bedsworth T, Barber A. Natural killer group 2D and CD28 receptors differentially activate mammalian/mechanistic target of rapamycin to alter murine effector CD8+ T-cell differentiation. *Immunology*. 2016;147:305-320.
21. Horng T, Bezbradica JS, Medzhitov R. NKG2D signaling is coupled to the interleukin 15 receptor signaling pathway. *Nat Immunol*. 2007;8:1345-1352.
22. Wensveen FM, Lenartić M, Jelenčić V, et al. NKG2D Induces Mcl-1 expression and mediates survival of CD8 memory T cell precursors via phosphatidylinositol 3-kinase. *J Immunol*. 2013;191:1307.
23. Jacquemin C, Martins C, Lucchese F, et al. NKG2D defines a subset of skin effector memory CD8 T cells with proinflammatory functions in vitiligo. *J Investig Dermatol*. 2020;140:1143-1153.e1145.
24. Zloza A, Kohlhapp FJ, Lyons GE, et al. NKG2D signaling on CD8+ T cells represses T-bet and rescues CD4-unhelped CD8+ T cell memory recall but not effector responses. *Nat Med*. 2012;18:422-428.
25. Thommen DS, Schumacher TN. T cell dysfunction in cancer. *Cancer Cell*. 2018;33:547-562.
26. Baitsch L, Baumgaertner P, Devêvre E, et al. Exhaustion of tumor-specific CD8+ T cells in metastases from melanoma patients. *J Clin Investig*. 2011;121:2350-2360.
27. Schietinger A, Philip M, Krisnawan VE, et al. Tumor-specific T cell dysfunction is a dynamic antigen-driven differentiation program initiated early during tumorigenesis. *Immunity*. 2016;45:389-401.
28. Mognol GP, Spreafico R, Wong V, et al. Exhaustion-associated regulatory regions in $CD8^+$ tumor-infiltrating T cells. *Proc Natl Acad Sci USA*. 2017;114:E2776.
29. Philip M, Fairchild L, Sun L, et al. Chromatin states define tumour-specific T cell dysfunction and reprogramming. *Nature*. 2017;545:452-456.
30. Henning AN, Roychoudhuri R, Restifo NP. Epigenetic control of CD8+ T cell differentiation. *Nat Rev Immunol*. 2018;18:340-356.
31. Scott AC, Dündar F, Zumbo P, et al. TOX is a critical regulator of tumour-specific T cell differentiation. *Nature*. 2019;571:270-274.
32. Khan O, Giles JR, McDonald S, et al. TOX transcriptionally and epigenetically programs CD8+ T cell exhaustion. *Nature*. 2019;571:211-218.

SUPPORTING INFORMATION

Additional supporting information may be found online in the Supporting Information section.

How to cite this article: Mojic M, Shitaoka K, Ohshima C, et al. NKG2D defines tumor-reacting effector $CD8^+$ T cells within tumor microenvironment. *Cancer Sci*. 2021;112:3484–3490. https://doi.org/10.1111/cas.15050